Free Shear Flows

mixing layer: $U = U_0 \tanh y/L$

Unstable $0 < k < k_N(Re)$

For large Re $0 < k < 1/L$

ie $\infty > \lambda > 2\pi L$

Long λ instability

$Re_{crit} = 0$

$c_{i\,max} = .2$ @ $kL = .4$

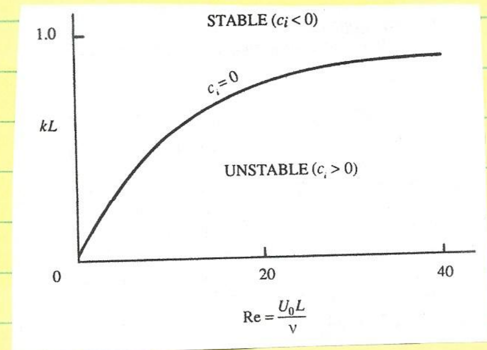

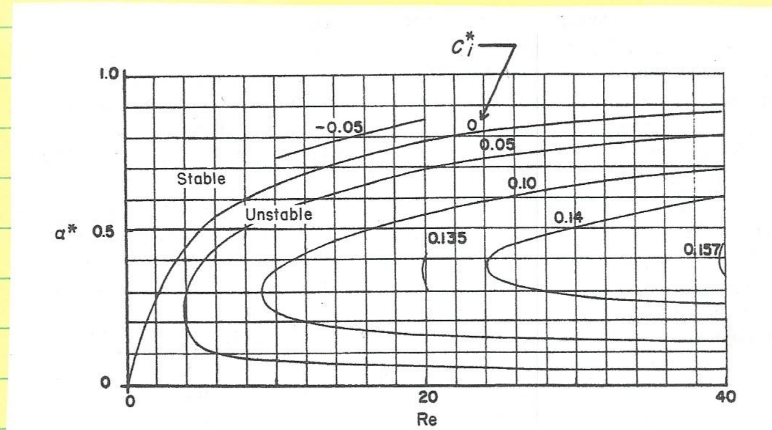

Figure 25.5 Curves of constant amplification $c_i^* = c_i \alpha L / U_0$ in the wavenumber $\alpha^* = \alpha L$ versus Re plane for a shear layer $u = U_0 \tanh(y/L)$. Neutral stability is given by $c_i^* = 0$. Viscosity makes the flow completely stable only at Re = 0. Reproduced with permission from Betchov and Szewczyk (1963). Graph courtesy of A. Szewczyk, Notre Dame University.

Transition U_1 to U_2 as seen observer moving $(U_1 + U_2)/2$

Long wave instability = KH instability

$\lambda <$ shear layer thickness stable

2D Jet : $U = U_0 \, \text{sech}^2 y$

$Re_{crit} \sim 4$ @ $\alpha \sim .2$

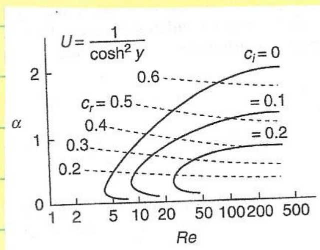

FIGURE 5-13
Eigenvalues for a two-dimensional jet. [*After Kaplan (1964).*]

2D Wake : $U = 1 + (U_0 - 1)\,\text{sech}^2 y$

$Re_{crit} = 4$

Wall-free free shear flows have inflection point i.e. inviscidly unstable. Smooth eigenfunctions (slowly varying). Zero order approximation viscous solution = regular perturbation expansion in powers $1/Re$

Instability appears as rolled up blobs of vorticity as per KH instability and easy to visualize vs wall bounded flows with unstable TS waves, which are difficult to observe.

Plane Poiseuille Flow: $U = 1 - y^2$

Inviscidly Stable

Linear viscous $Re_{cr} = 5780$

Non-linear viscous (finite amplitude perturbations)

$Re_{cr} = 2510$, which has better agreement EFD

μ de-stabilizes the flow!

In contrast flows with inflection points

Complex viscous flow analysis requires singular perturbation expansions. Eigenfunctions are fast varying in boundary layer near walls and critical layers near $U = c_r$.

Physically instability exhibited as waves called Tollmien-Schlichting waves.

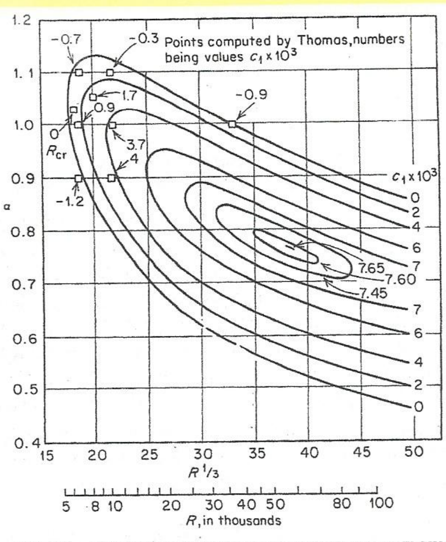

FIGURE 5. STABILITY DIAGRAM FOR PLANE POISEUILLE FLOW. [*S. F. Shen, J. Aeron. Sci.*, **21** (1954), *by permission of the American Institute of Aeronautics and Astronautics.*]

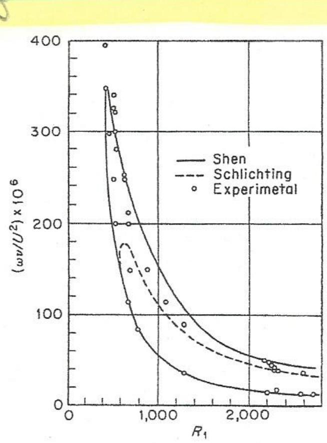

FIGURE 6. NEUTRAL-STABILITY CURVE FOR BLASIUS FLOW. R_1 IS THE REYNOLDS NUMBER BASED ON THE DISPLACEMENT THICKNESS, AND ω IS THE CIRCULAR FREQUENCY OF OSCILLATION. [*S. F. Shen, J. Aeron. Sci.*, **21** (1954), *by permission of the American Institute of Aeronautics and Astronautics.*]

Plane Couette Flow: $U = \Gamma y$

Contrary EFD linear μ theory shows stable all Re

Pipe Flow: $U = U = 1 - r^2$

Re per plane Couette flow stable both $\mu = 0$ & $\neq 0$ w/ contrary EFD

$Re_{crit} \sim 3000$

careful EFD $Re_{crit} \sim 50{,}000$

Transition attributed: (1) finite amplitude disturbance

(2) entrance effects due BL

(3) " " due $\underline{\omega}$

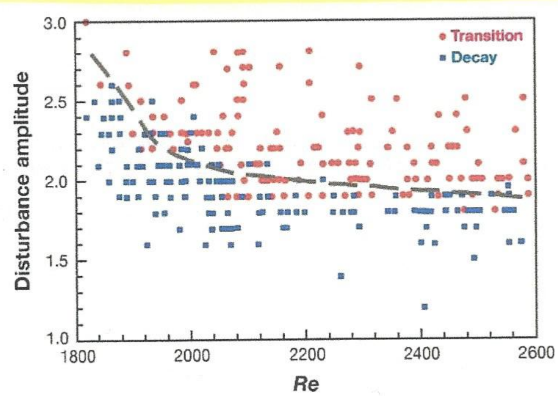

Figure 1

Transition experiments by Darbyshire & Mullin (1995). Disturbances were introduced at a distance 70 diameters downstream of the inlet, and their status was probed at another 120 diameters downstream, delayed with the mean advection time. Depending on whether the perturbation was still present or not, a point was marked "transition" or "decay." The amplitude of the perturbations is proportional to the injected fluid volume. For more details, see Darbyshire & Mullin (1995). Redrawn after Darbyshire & Mullin (1995).

Boundary Layers With Pressure Gradient

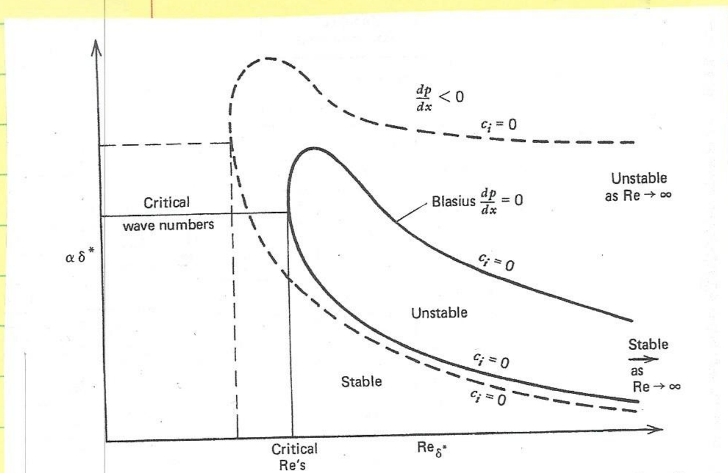

Figure 25.4 General shape of the neutral stability curve (locus of $c_i = 0$ in wavenumber–Reyno number space) for a Blasius boundary layer and for layers with adverse pressure gradients.

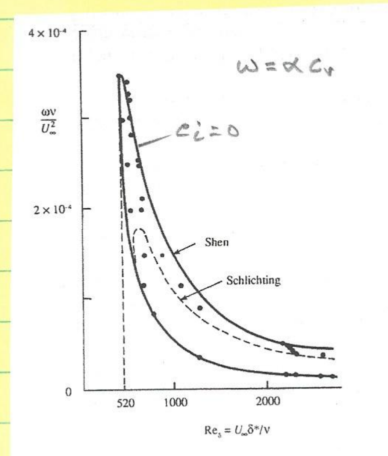

EFD Schubauer and Skramstad (1947)

Low Re stable all α due μ

Large Re stable all α for $p_x = 0$ due no inflection point

Unstable in "thumb curve" due TS waves

$Re_{crit} = 520 \quad \alpha\delta^* = .3 \quad L = 2\pi/\alpha = \frac{2\pi\delta^*}{.3}$

$= 18\delta^*$

$= 6\delta$!

BL stable short wave, but unstable long waves

BL with adverse p_x have inflection point so unstable at large Re. TS waves unstable smaller λ & $Re_{crit} \downarrow$

Table 25.1 Critical Reynolds Number for Falkner–Skan Boundary Layers

m=1 stagnation
m=0 Blasius
= -.0904 separation

$\beta_1 = 2m/(m+1)$	1	0.8	0.6	0.5	0.4	0.3	0.2
m	1	0.667	0.429	0.333	0.250	0.176	0.111
$H = \delta^*/\theta$	2.216	2.24	2.274	2.297	2.325	2.362	2.411
Re_crit	12490	10920	8890	7680	6230	4550	2830
β_1	0.1	0.05	0	−0.05	−0.1	−0.14	−0.1988
m	0.053	0.026	0	−0.024	−0.048	−0.065	−0.0904
$H = \delta^*/\theta$	2.481	2.529	2.591	2.676	2.801	2.963	4.029
Re_crit	1380	865	520	318	199	138	67

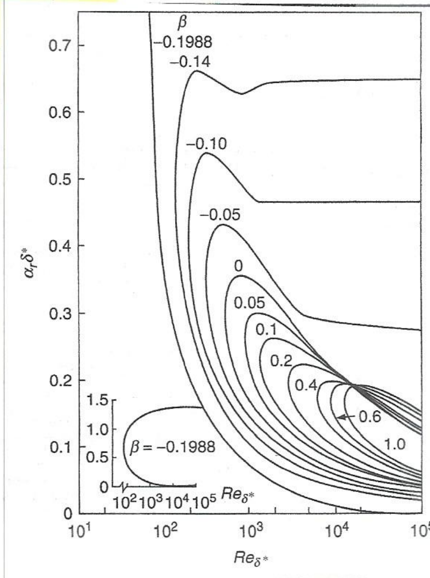

FIGURE 5-7
Neutral stability curves for Falkner–Skan boundary-layer profiles. [*After Wazzan et al. (1968b).*]

TABLE 5-1
Spatial stability parameters for Falkner–Skan profiles

β	$Re_{\delta^*,\text{crit}}$	$Re_{\hat{\theta},\text{crit}}$	$c_{i,\max}$	$\left(-\frac{\alpha\delta^*}{Re_{\delta^*}}\right)_{\max} \times 10^7$
+1.0	12,490	5,636	0.0065	1.14
0.8	10,920	4,874	0.0070	1.35
0.6	8,890	3,909	0.0075	1.67
0.5	7,680	3,344	0.0080	1.92
0.4	6,230	2,679	0.0085	2.42
0.3	4,550	1,927	0.0095	3.45
0.2	2,830	1,174	0.0104	6.0
0.1	1,380	556	0.0129	15.7
0.05	865	342	0.0154	32
0.0	520	201	0.0196	74
−0.05	318	119	0.0275	186
−0.1	199	71	0.0388	450
−0.14	138	47	0.0525	963
−0.1988	67	17	0.12	5,600

Source: Computations by Wazzan et al. (1968*b*).

Table 25.2 Stability Characteristics

Flow	$U(y)/U_0$	$U_0L/\nu = \text{Re}_c$	$\alpha_c L = \alpha^*$	$0 - \alpha^*_\infty$ Inviscid	Remarks
Shear layer	$\tanh(y/L)$	0	0	0–1.0	Kelvin–Helmholtz, Re → ∞
Jet	$\text{sech}^2(y/L)$	4	0.2	0–2.0	Even mode
Falkner–Skan separating profile	$\beta = -0.199$	64	1.24	0–0.8	$L = \delta^*$
Blasius	$\beta = 0$	520	0.30	0	$L = \delta^*$
Stagnation	$\beta = 1$	14,000		0	$L = 8^*$
Flow into a sink	$\beta \to \infty$	21,700	0.17	0	$L = \delta^*$
Poiseuille (plane)	$1 - (y/L)^2$	5,780	1.02	0	L = half-width
Poiseuille (cylindrical)	$1 - (r/R)^2$	∞		0	Stable
Couette (plane)	y/L	∞		0	Stable

TABLE 12.1 Linear Stability Results of Common Viscous Parallel Flows

Flow	$U(y)/U_0$	Re_{cr}	Remarks
Jet	$\text{sech}^2(y/L)$	4	
Shear layer	$\tanh(y/L)$	0	Always unstable
Blasius		520	Re based on δ^*
Plane Poiseuille	$1 - (y/L)^2$	5780	L = half-width
Pipe flow	$1 - (r/R)^2$	∞	Always stable
Plane Couette	y/L	∞	Always stable

EFD Validation Boundary Layer Instability

Usually EFD followed by AFD & CFD = numerical but in this case AFD & numerical; since, EFD difficult due to need low levels free stream turbulence and mechanism to generate normal mode wave disturbance ie vibrating ribbon such that natural transition occurs due to TS waves. Otherwise large disturbances cause bypass or forced transition.

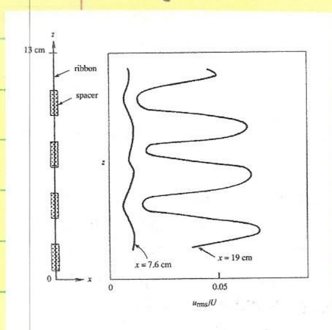

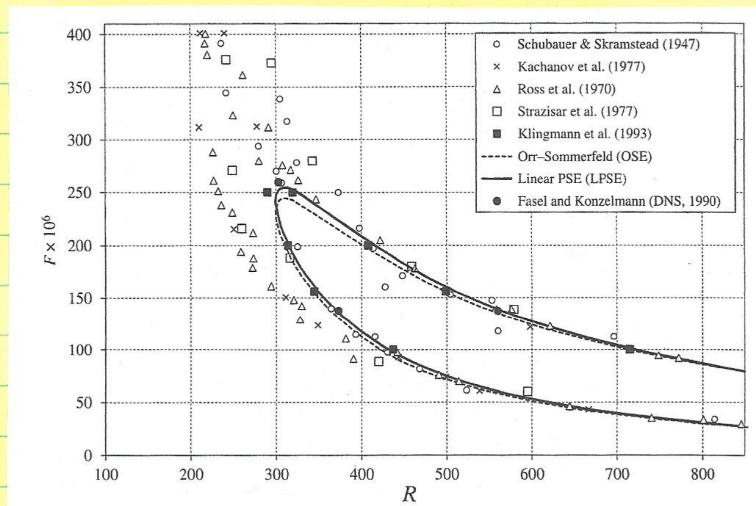

Figure 25.7 Modern Blasius boundary layer results from Saric (2013); $F = 2\pi f\nu/U_0^2 \times 10^6$ and $R = \sqrt{U_0 x/\nu} = \sqrt{\mathrm{Re}_x}$. Solid line is parabolized stability equations (PSE) calculations from Bertolotti et al. (1992) Dashed line is solution of the Orr–Sommerfeld equation (OSE) from Wazzan et al. (1968). The [•] symbols are direct numerical simulation (DNS) calculations of Fasel and Konzelmann (1990). Experimental results are Schubauer and Skramstead (1947) [∘], Ross, Barnes, Burns, and Ross (1971) [Δ] Kachanov et al. (1977) [×], Strazisar et al. (1977) [□] and Klingmann et al. (1993) [■]

EFD $Re_{\delta^* trans} \sim 3000$

theory $Re_{crit} = 520$

EFD $Re_{crit} = 450$ $\ll Re_{trans}$ due slow growth process $20 \to 30$ and nonlinear etc.

Modern results try explain this difference due: BL growth, weak adverse p_x.